

CAM 1178

A comparison of two methods for solving the inverse scattering problem for acoustic waves in an inhomogeneous medium *

David Colton and Peter Monk

Department of Mathematical Sciences, University of Delaware, Newark, DE 19716, United States

Received 25 February 1991

Revised 28 June 1991

Abstract

Colton, D. and P. Monk, A comparison of two methods for solving the inverse scattering problem for acoustic waves in an inhomogeneous medium, *Journal of Computational and Applied Mathematics* 42 (1992) 5–16.

A comparison is made of two methods for solving the inverse scattering problem for acoustic waves in an inhomogeneous absorbing medium. These methods were recently introduced by Colton, Kirsch and Monk and are based on considering a weighted average of the far-field data instead of the far-field data itself. The comparison is based on numerical examples for the special case of spherically stratified media.

Keywords: Inverse scattering, acoustic waves.

1. Introduction

This paper is concerned with the inverse scattering problem for time harmonic acoustic waves in an inhomogeneous medium. There are three basic (nonlinear) methods for solving this problem, all of which are based on the Lippmann–Schwinger equation and nonlinear optimization techniques, but each of which differs in the type of constraint imposed in order to determine the index of refraction. We shall briefly describe these three methods in the following section, only noting here that two of them employ an averaging process such that the final optimization scheme is independent of the number of plane waves used to probe the medium. It is these two methods that we shall compare in this paper, noting that the first (and simpler) of these two methods requires that the medium be absorbing in order to avoid the presence of what are called transmission eigenvalues. The aim of this paper is to consider

Correspondence to: Prof. D.L. Colton, Department of Mathematical Sciences, University of Delaware, 501 Kirkbride Office, Newark, DE 19716, United States.

* This research was supported in part by grants from the Air Force Office of Scientific Research and the National Science Foundation.

numerical examples involving spherically stratified media in order to answer the following questions.

- (1) How much absorption is necessary in order for the first method to be reliable?
- (2) Given sufficient absorption for the first method to be reliable, which of the two methods gives the better reconstruction?
- (3) If k is the wave number and a is a typical dimension of the inhomogeneous medium, how large does ka have to be in order to get accurate reconstructions?

The answers to these questions are contained in the analysis which follows. However, we can briefly summarize our results by saying that the amount of absorption that is necessary for the first method to be reliable depends on the order of the averaging procedure used and, when sufficient absorption is present, both methods provide comparable accuracy in reconstructing the index of refraction. Furthermore, ka must be larger than around 5 or 6 for accurate reconstructions to be attainable in our examples. In particular, this explains the poor reconstructions obtained in [5]. Based on the experiments performed here, and similar experiments in the case of the inverse obstacle problem [9], we would hazard to predict that each of the three methods for solving the inverse scattering problem has comparable accuracy, but none of them will be better than the others in all circumstances. Here we wish to emphasize that in order to avoid trivial inversion of finite-dimensional problems, it is crucial in using examples with synthetic data that the forward solver have no connection to the inverse solver under consideration or, at least, every effort is made to minimize any connection that does exist. Unfortunately, not all of the numerical examples that appear in the literature follow this obvious requirement.

2. The inverse scattering problem

We consider the propagation of an acoustic time harmonic plane wave through an absorbing inhomogeneous medium of compact support. Let $c(x)$ denote the local speed of sound and $\gamma(x)$ the absorption where $x \in \mathbb{R}^3$. We assume that $c(x) = c_0$ and $\gamma(x) = 0$ for $r = |x| \geq a$, where c_0 is a positive constant. Then, if ω is the frequency of the incident wave, α , $|\alpha| = 1$, its direction of propagation, $k = \omega/c_0$ the wave number and

$$n(x) = \left(\frac{c_0}{c(x)} \right)^2 + i \frac{\gamma(x)}{k}$$

the index of refraction, we want to determine the velocity potential $u(x)$ of the total field such that

$$\Delta_3 u + k^2 n(x) u = 0, \quad \text{in } \mathbb{R}^3, \quad (2.1)$$

$$u(x) = \exp[ikx \cdot \alpha] + u^s(x), \quad (2.2)$$

$$\lim_{r \rightarrow \infty} r \left(\frac{\partial u^s}{\partial r} - iku^s \right) = 0, \quad (2.3)$$

where $u^s(x)$ denotes the velocity potential of the scattered field and the Sommerfeld radiation condition (2.3) is assumed to hold uniformly for $\hat{x} = x/|x|$ on the unit sphere Ω . We shall assume that $n(x)$ is continuously differentiable.

The scattering problem (2.1)–(2.3) is equivalent to the *Lippmann–Schwinger equation*

$$u(x) = \exp[ikx \cdot \alpha] - k^2 \int_B \int \Phi(x, y) m(y) u(y) dy, \quad (2.4)$$

where $m(x) = 1 - n(x)$, B is the support of $m(x)$ and

$$\Phi(x, y) = \frac{\exp[ik|x-y|]}{4\pi|x-y|}.$$

Using the unique continuation principle, it can easily be shown that there exists a unique solution of (2.4) in $C(\bar{B})$ for any $k > 0$ and furthermore, letting r tend to infinity in (2.4), we have that

$$u^s(x) = \frac{\exp[ikr]}{r} F(\hat{x}; k, \alpha) + O\left(\frac{1}{r^2}\right),$$

where the *far-field pattern* $F(\hat{x}; k, \alpha)$ is defined by

$$F(\hat{x}; k, \alpha) = -\frac{k^2}{4\pi} \int_B \int \exp[-ik\hat{x} \cdot y] m(y) u(y) dy. \quad (2.5)$$

The *inverse scattering problem* is to determine $m(x)$ (i.e., the sound speed $c(x)$ and absorption $\gamma(x)$) from the far-field pattern $F(\hat{x}; k, \alpha)$ for $\hat{x} \in \Omega$ and a finite set of values of k and α .

As mentioned in the Introduction, there are three methods for solving the inverse scattering problem, all of which are based on the Lippmann–Schwinger equation and nonlinear optimization methods (we are not considering linear approaches, such as those based on the Born or Rytov approximations). The first method is to find a solution $m(x)$ and $u(x)$ of the Lippmann–Schwinger equation (2.4) such that $m(x)$ and $u(x)$ satisfy the constraint (2.5). This is done by reformulating (2.4) and (2.5) as a nonlinear optimization problem subject to a priori constraints on $m(x)$ such that the optimization problem has a solution that depends continuously on the data. Variations of this approach have been used in [8,10,12–18]. There are, of course, important differences in the practical implementation in each of these papers, for example, the far-field constraint (2.5) is sometimes replaced by an analogous near-field condition and the optimization scheme is numerically solved by different methods, viz. successive overrelaxation, sinc basis moment methods, steepest descent, etc. However, in all of these cases the underlying cost functional is essentially the same.

A second approach to solving the inverse scattering problem was introduced in [4] and given a theoretical basis in [2]. This method (as well as the third approach to be discussed shortly) has the advantage of being able to increase the number of incident fields without increasing the cost of solving the inverse problem. We shall henceforth refer to this approach as *Method A*. In this approach, we first try to choose $g_{pq} \in L^2(\Omega)$ such that

$$\int_{\Omega} F(\hat{x}; k, \alpha) g_{pq}(\hat{x}) ds(\hat{x}) = -\frac{i^{p+1}}{k} Y_p^q(\alpha) \quad (2.6)$$

for the given set of incident directions α where Y_p^q is a spherical harmonic and $0 \leq p \leq P$, $-p \leq q \leq p$. Having determined $g_{pq}(\hat{x})$, we construct the *Herglotz wave function*

$$v_{pq}(x) = \int_{\Omega} g_{pq}(\hat{y}) \exp[-ikx \cdot \hat{y}] ds(\hat{y}), \quad (2.7)$$

and then seek a solution $m(x)$ and $w_{pq}(x)$ of the Lippmann–Schwinger equation

$$w_{pq}(x) = v_{pq}(x) - k^2 \int_B \Phi(x, y) m(y) w_{pq}(y) dy \quad (2.8)$$

such that $m(x)$ and $w_{pq}(x)$ satisfy the constraint

$$-k^2 \int_B \Phi(x, y) m(y) w_{pq}(y) dy = h_p^{(1)}(kr) Y_p^q(\hat{x}) \quad (2.9)$$

for $|x| = b > a$ where $h_p^{(1)}$ is a spherical Hankel function of the first kind. (Note that (2.8) and (2.9) imply that $w_{pq}(x) = v_{pq}(x) + h_p^{(1)}(kr) Y_p^q(\hat{x})$ for $|x| \geq b$ and (2.6) now follows from (2.5) and Green's formula.) Reformulating (2.6)–(2.9) as a constrained nonlinear optimization problem now yields a solution to the inverse scattering problem, provided $\gamma(x) > 0$ for $|x| < a$, i.e., the medium is absorbing. If $\gamma(x) = 0$ for $|x| < a$, there can exist *transmission eigenvalues* such that the solution of the ill-posed integral equation (2.6) is not unique and these transmission eigenvalues can contaminate the numerical implementation of this method of solving the inverse scattering problem [3,4]. Numerical examples using Method A can be found in [4,5] for the case when there is no absorption and $P = 0$ (as noted in the Introduction, the numerical results of [5] are poor due to the fact that in this paper it was necessary to keep $ka < 4$ due to limitations in the finite-element package that was used).

A third method for solving the inverse scattering problem which still uses averaging as in (2.6), but avoids the problem of transmission eigenvalues, was introduced in [6,7]. We shall call this approach *Method B*. To describe this method, we first define $h(x)$ to be the solution of the exterior impedance boundary value problem

$$\Delta_3 h + k^2 h = 0, \quad \text{in } \mathbb{R}^3 \setminus \bar{B}_0, \quad (2.10)$$

$$h(x) = \exp[ikx \cdot \alpha] + h^s(x), \quad (2.11)$$

$$\frac{\partial h}{\partial r} + i\lambda h = 0, \quad \text{on } \partial B_0, \quad (2.12)$$

$$\lim_{r \rightarrow \infty} r \left(\frac{\partial h^s}{\partial r} - ikh^s \right) = 0, \quad (2.13)$$

where λ is a constant chosen such that a solution to (2.10)–(2.13) exists and $B_0 = \{x: |x| < b\}$ where $b > a$. We now denote the far-field pattern of $h^s(x)$ by $F_\lambda(\hat{x}; k, \alpha)$, i.e.,

$$h^s(x) = \frac{\exp[ikr]}{r} F_\lambda(\hat{x}; k, \alpha) + O\left(\frac{1}{r^2}\right),$$

and try to choose $g_{pq} \in L^2(\Omega)$ such that

$$\int_\Omega [F(\hat{x}; k, \alpha) - F_\lambda(\hat{x}; k, \alpha)] g_{pq}(\hat{x}) ds(\hat{x}) = -\frac{i^{p+1}}{k} Y_p^q(\alpha) \quad (2.14)$$

for the given set of incident directions α where $0 \leq p \leq P$, $-p \leq q \leq p$. Having determined $g_{pq}(\hat{x})$, we construct the Herglotz wave function $v_{pq}(x)$ defined by (2.7) and then seek a solution $m(x)$ and $w_{pq}(x)$ of the Lippmann–Schwinger equation (2.8) such that $m(x)$ and $w_{pq}(x)$ satisfy the constraint

$$\left(\frac{\partial}{\partial r} + i\lambda \right) (w_{pq}(x) - h_p^{(1)}(kr) Y_p^q(\hat{x})) = 0, \quad \text{on } \partial B_0. \quad (2.15)$$

(Note that if $h_{pq}(x)$ is the solution of (2.10)–(2.13) with $\exp[ikx \cdot \alpha]$ replaced by $v_{pq}(x)$ and if $w_{pq}(x)$ is defined by (2.8), then from (2.14) and the reciprocity principle we have that $w_{pq}(x) - h_{pq}(x) = h_p^{(1)}(kr)Y_p^q(\hat{x})$ for $|x| \geq b$, i.e., (2.15) is valid.)

Reformulating (2.14), (2.7), (2.8) and (2.15) as a constrained nonlinear optimization problem now yields a solution to the inverse scattering problem. As previously mentioned, an advantage of Method B over Method A is that by choosing λ appropriately the problem of transmission eigenvalues can be avoided. In particular, if $\text{Im } n(x) = 0$ we can choose $\lambda > 0$, whereas if $\text{Im } n(x) \neq 0$ we can choose $\lambda = 0$. Preliminary numerical examples using Method B can be found in [6,7].

3. The spherically stratified medium

To allow a rapid comparison of Methods A and B discussed above, we shall apply the methods to reconstruct a spherically stratified profile. By a spherically stratified profile we mean that $m(x)$ is a priori known to depend only on $r = |x|$.

First let us consider the forward problem. As in [7], when $m(x) = m(r)$ the total field $u(x)$ in (2.1)–(2.3) can be written

$$u(x) = \sum_{p=0}^{\infty} u_p(r) P_p(\cos \theta), \quad (3.1)$$

where

$$\cos \theta = \frac{x \cdot \alpha}{r}.$$

Using (3.1) in (2.4), it can be shown [1, pp. 41–42] that $u_p(r)$ satisfies

$$u_p(r) = i^p(2p+1)j_p(kr) - ik^3 \int_0^{\alpha} K_p(r, \rho) m(\rho) u_p(\rho) \rho^2 d\rho, \quad (3.2)$$

where

$$K_p(r, \rho) = \begin{cases} j_p(kr)h_p^{(1)}(k\rho), & \text{if } \rho \leq r, \\ j_p(k\rho)h_p^{(1)}(kr), & \text{if } \rho > r. \end{cases} \quad (3.3)$$

Here j_p and $h_p^{(1)}$ are, respectively, the p th-order spherical Bessel and first-kind Hankel functions. Then from (2.5),

$$F(\hat{x}; k, \alpha) = \sum_{p=0}^{\infty} f_p(k) P_p(\cos \theta), \quad (3.4)$$

where

$$f_p(k) = (-i)^{p+2} k^2 \int_0^{\alpha} j_p(k\rho) m(\rho) u_p(\rho) \rho^2 d\rho. \quad (3.5)$$

The Fourier coefficients of the far-field pattern $\{f_p(k)\}_{p=0}^{\infty}$ can thus be found by solving (3.2) and using (3.5).

Turning now to the inverse problem in the case when $m(x) = m(r)$, we discuss Method A first. From (2.6) and (3.4),

$$g_{pq}(\hat{x}) = i^{p-1} \frac{(2p+1)Y_p^q(\hat{x})}{4\pi k f_p(k)}. \quad (3.6)$$

As is to be expected, g_{pq} depends on q in a way that is independent of F and hence, independent of m . Thus we only consider the case $q = 0$, and define $g_p(\hat{x}) \equiv g_{p0}(\hat{x})$. Having computed g_p , we can compute $v_p(x) \equiv v_{p0}(x)$. From (2.7) and (3.6),

$$v_p(x) = -i \frac{(2p+1)j_p(kr)}{k f_p(k)} \sqrt{\frac{2p+1}{4\pi}} P_p(\cos \theta). \quad (3.7)$$

Next we need to compute $w_{p0}(x)$ which satisfies the Lippmann–Schwinger equation (2.8). From (3.7), if we define

$$w_{p0}(x) = w_p(r) \sqrt{\frac{2p+1}{4\pi}} P_p(\cos \theta), \quad (3.8)$$

then $w_p(r)$ satisfies the following equation analogous to (3.2):

$$w_p(r) = -i \frac{(2p+1)j_p(kr)}{k f_p(k)} - i k^3 \int_0^a K_p(r, \rho) m(\rho) w_p(\rho) \rho^2 d\rho. \quad (3.9)$$

Finally, we must satisfy the constraint (2.9). If B has radius b , then from (2.8) and (2.9),

$$w_{pq} - v_{pq} = h_p^{(1)}(kr) Y_p^q(\hat{x}), \quad \text{on } \partial B, \quad (3.10)$$

so by (3.7) and (3.8),

$$w_p(b) + i \frac{(2p+1)j_p(kb)}{k f_p(k)} = h_p^{(1)}(kb). \quad (3.11)$$

Noting also that by (2.8), $w_{pq} - v_{pq}$ satisfies the exterior problem for the Helmholtz equation outside B , and using the unique continuation property of solutions of the Helmholtz equation, we see that

$$\frac{\partial}{\partial r} (w_{pq} - v_{pq}) = \frac{\partial}{\partial r} (h_p^{(1)}(kr) Y_p^q(\hat{x})), \quad \text{on } \partial B.$$

Hence, in the spherically stratified case,

$$\frac{\partial}{\partial r} \left(w_p(r) + i \frac{(2p+1)j_p(kr)}{k f_p(k)} \right) \bigg|_{r=b} = \left(\frac{\partial}{\partial r} h_p^{(1)}(kr) \right) \bigg|_{r=b}. \quad (3.12)$$

To summarize, Method A consists of finding $m(r)$ and $w_p(r)$ for $0 \leq p < \infty$ such that (3.9), (3.11) and (3.12) hold for each p and for k in some interval of k values.

A similar derivation to that given above can be carried out for Method B, and was presented in [7]. We summarize the results here. Let

$$\gamma_p(k) = \frac{i(2p+1)}{k} \left(\frac{(\partial/\partial r)j_p(kr) + i\lambda j_p(kr)}{(\partial/\partial r)h_p^{(1)}(kr) + i\lambda h_p^{(1)}(kr)} \right) \bigg|_{r=b}. \quad (3.13)$$

$\{\gamma_p(k)\}_{p=0}^\infty$ are the Fourier coefficients of F_λ (see (2.10)–(2.13)). Then we define

$$a_p(k) = -\frac{i}{k[f_p(k) - \gamma_p(k)]}, \quad 0 \leq p \leq \infty.$$

With these definitions $w_p(r)$ satisfies the integral equation

$$w_p(r) = a_p(k)(2p+1)j_p(kr) - ik^3 \int_0^a K_p(r, \rho) m(\rho) w_p(\rho) \rho^2 d\rho. \quad (3.14)$$

Using $w_p(r)$, (2.15) becomes

$$\left(\frac{\partial}{\partial r} + i\lambda \right) (w_p(r) - h_p^{(1)}(kr))|_{r=b} = 0. \quad (3.15)$$

Thus, for Method B, we must find $w_p(r)$, $0 \leq p < \infty$, and $m(r)$ such that (3.14), (3.15) are satisfied for an interval of k values.

4. Numerical results

In this section we shall present some numerical results for Methods A and B applied to the inverse problem for a spherically stratified medium. As in previous papers [4,6,7], we shall use synthetic far-field data obtained by approximating (3.2). We then apply Methods A and B to reconstruct the profile.

To discretize (3.2), we use an N_f point Nyström method to approximate $w_p(r)$ [11]. Then we compute the far-field pattern for

$$k = k_j = k_{\min} + (k_{\max} - k_{\min}) \left(\frac{j-1}{N_k - 1} \right), \quad 1 \leq j \leq N_k,$$

by using the trapezoidal rule with N_f points to discretize (3.5). Thus the data for the inverse solver is an approximation to $\{f_p(k_j)\}$, $0 \leq p \leq P$, $1 \leq j \leq N_k$.

To discretize $m(r)$ we use a cubic spline basis with N_m equally spaced knots in $[0, a]$ under the constraints that $m(a) = m'(0) = 0$. This implies that the expansion for $m(r)$ has N_m free parameters that must be computed via an appropriate inverse algorithm.

To implement Methods A and B, we approximate, respectively, (3.9) and (3.14) using Nyström's method with N_i equally spaced quadrature points on $[0, a]$. The approximate solution to (3.9) or (3.14) can be continued away from the Nyström points by using an N_i point trapezoidal rule to approximate the integral in (3.9) or (3.14). Let $w_p^a(r, \tilde{m}, k)$ represent the Nyström solution of either (3.9) or (3.14) with m replaced by an arbitrary function \tilde{m} .

For Method A, we work with (3.9) and (3.12). The inverse algorithm then consists of finding a discrete profile m^* such that

$$F_{p,j}^A(\tilde{m}) \equiv \frac{\partial}{\partial r} \left[w_p^a(r, \tilde{m}, k_j) + i \frac{(2p+1)j_p(k_j r)}{k_j f_p(k_j)} - h_p^{(1)}(k_j r) \right] \Big|_{r=b} \quad (4.1)$$

is as small as possible when $\tilde{m} = m^*$ for each j and p .

Similarly, from (3.15), Method B consists of finding a discrete profile m^* such that

$$F_{p,j}^B(\tilde{m}) = \left(\frac{\partial}{\partial r} + i\lambda \right) \left(w_p^a(r, \tilde{m}, k_j) - h_p^{(1)}(k_j r) \right) \Big|_{r=b} \quad (4.2)$$

is as small as possible when $\tilde{m} = m^*$ for each p and j .

Since the inverse problem is ill-posed, we use a Tikhonov regularization technique to minimize (4.1) or (4.2). Let

$$J_\omega(\tilde{m}) = \frac{1}{N_k(P+1)} \sum_{p=0}^P \sum_{j=1}^{N_k} |F_{p,j}(\tilde{m})|^2 + \omega^2 \|m'\|_{L^2(0,a)}^2, \quad (4.3)$$

where $F_{p,j}$ is given by either (4.1) or (4.2), and ω is a regularization parameter. The approximate solution m^* for either Method A or B is obtained by minimizing $J_\omega(\tilde{m})$ over the spline space for \tilde{m} with $F_{p,j}(\tilde{m})$ replaced by (4.1) for Method A or by (4.2) for Method B. Since \tilde{m} is given by a cubic spline, the minimization of (4.3) is a finite-dimensional optimization problem and we use a Levenberg–Marquardt method to implement the optimization scheme.

Before presenting some numerical examples, some comments are in order regarding the design of numerical tests for inverse algorithms. Care must be taken that interactions between the inverse and forward solvers do not result in excessively optimistic predictions regarding the stability or accuracy of an inverse algorithm. For example, if (2.4) and (2.5) are discretized and used to generate far-field data for a given profile, and the same discretization is used to solve the inverse problem, it is possible that the essential ill-posedness of the inverse problem may not be evident. This is avoided in our example, since Methods A and B, using (2.6) or (2.14), avoid the use of (2.5) to process the far-field data.

A similar problem can occur if the subspace containing the discrete coefficient \tilde{m} contains or conforms with the exact solution. This problem is particularly acute if a piecewise-constant approximation is used to approximate a discontinuous coefficient. If the grid lines for the discrete coefficient correspond to actual discontinuities in the exact solution, the inverse solver may again show spurious accuracy. In particular, one cannot choose the mesh consistent with the profile to be reconstructed. In our examples, we use a cubic spline basis for approximating m , and choose target profiles that are not contained in the cubic spline space.

Now let us discuss a few numerical examples. The first two examples were used in [7], and our results suggest that when both methods A and B work satisfactorily, the error in the reconstruction is approximately the same in both cases.

Example 1. This was [7, Example 3]. We take

$$\left(\frac{c}{c_0(\tau)} \right)^2 = 1 + \frac{1}{2} \cos\left(\frac{\gamma}{2}\pi r\right), \quad 0 \leq r \leq 1 = a, \quad (4.4)$$

$$\gamma(r) = \frac{1}{2}(1-r)^2(1+2r). \quad (4.5)$$

The absorption $\gamma(r)$ is a cubic spline, but $(c/c_0(r))^2$ is not. We use the same values of the parameters as in [7]. In particular, $k_{\min} = 1$, $k_{\max} = 7$, $N_f = 513$, $N_i = 150$ and $\lambda = 0$. The solution is computed for the regularization parameter $\omega = 0.001$ by first computing m^* for $\omega = 0.1$, taking as initial guess for the coefficients of m the value -0.3 as in [7]. The solution

Table 1
Results for Methods A and B used to reconstruct (4.4) and (4.5)

P	Method A		Method B	
	$N_k = 9$	$N_k = 15$	$N_k = 9$	$N_k = 15$
0	26.5	26.2	27.2	27.1
1	13.2	13.3	41.0	40.3
2	9.59	9.66	12.0	11.7
3	9.35	8.66	11.7	11.8

Table 2
A table of relative L^2 error (4.6) (as a percentage) in the reconstruction of (4.7) and (4.8)

P	Method A		Method B	
	$N_k = 9$	$N_k = 15$	$N_k = 9$	$N_k = 15$
0	11.2	10.5	11.1	10.8
1	10.0	9.85	10.5	11.2
2	111.0	9.51	10.1	9.88
3	131.0	9.38	9.67	9.49

for $\omega = 0.1$ is used as an initial guess for $\omega = 0.01$ and this solution is used as initial guess for $\omega = 0.001$. We report only results for $\omega = 0.001$. The crude continuation technique just described would be useful in practice for checking convergence (or independence of ω) and for allowing a poor initial guess. In Table 1 we report the relative L^2 error in the reconstructions defined by

$$\left(\frac{\|\operatorname{Re}(n^* - n_e)\|_{L^2(0,a)}^2 + k^2 \|\operatorname{Im}(n^* - n_e)\|_{L^2(0,a)}^2}{\|\operatorname{Re}(n_e)\|_{L^2(0,a)}^2 + k^2 \|\operatorname{Im}(n_e)\|_{L^2(0,a)}^2} \right)^{1/2}. \quad (4.6)$$

Here n_e is the exact solution (in this case given by (4.4) and (4.5)) and n^* is the approximate reconstruction. In Table 1 we give the relative L^2 error (see (4.6)) expressed as a percentage. The two methods are of comparable accuracy except when $P = 1$, when Method A is markedly superior to Method B. The results reported for Method B are from [7].

Example 2. Our next example is a discontinuous profile:

$$\left(\frac{c_0}{c(r)} \right)^2 = \begin{cases} 3.5, & \text{if } r < 0.5, \\ 1, & \text{if } r \geq 0.5, \end{cases} \quad (4.7)$$

$$\gamma(r) = 0.3(1 + \cos(3\pi r)), \quad 0 \leq r \leq 1 = a. \quad (4.8)$$

This was [7, Example 2]. In this case neither $(c_0/c(r))^2$ nor $\gamma(r)$ are cubic spline functions. Table 2 shows results for reconstructing this profile (parameters are as in Example 1). When both methods work satisfactorily, they possess similar errors, and both methods can approximate discontinuous profiles. However, Method A is somewhat less robust than Method B and fails to work in two cases. This failure may be due to insufficient absorption γ to stabilize Method A. The effect of absorption on the reconstruction is investigated further in the next example.

Example 3. In this example we allow the maximum value of the absorption to be variable:

$$\left(\frac{c}{c_0(r)} \right)^2 = 1 + \frac{1}{2} \cos\left(\frac{5}{2}\pi r\right), \quad 0 \leq r \leq 1 = a, \quad (4.9)$$

$$\gamma(r) = \frac{1}{2} \gamma_{\max} (1 - r)^2 (1 + 2r), \quad 0 \leq r \leq 1. \quad (4.10)$$

Table 3

A table of the relative L^2 error (4.6) (as a percentage) in the reconstruction of (4.9) and (4.10) as γ_{\max} varies

γ_{\max}	Method A				Method B			
	$P=0$	$P=1$	$P=2$	$P=3$	$P=0$	$P=1$	$P=2$	$P=3$
0.0	107.0	87.4	53.5	52.0	5.89	2.44	2.59	2.26
0.01	109.0	88.6	2.72	25.9	—	—	—	—
0.025	105.0	89.9	3.88	2.53	—	—	—	—
0.05	213.0	96.5	2.73	2.56	—	—	—	—
0.1	124.0	165.0	2.75	2.62	5.87	2.44	2.59	2.26
0.15	6.24	320.0	2.78	2.68	—	—	—	—
0.2	6.24	2.60	2.80	2.74	5.81	2.44	2.58	2.26
0.3	6.25	2.65	2.83	2.83	5.73	2.44	2.58	2.24
0.4	6.21	2.70	2.86	2.92	5.62	2.43	2.57	2.25
0.5	6.15	2.76	2.90	3.00	5.50	2.43	2.56	2.25

When $\gamma_{\max} = 0$, we obtain [7, Example 1]. To reconstruct (4.9) and (4.10), we take $N_f = 129$, $N_k = 15$ and $N_i = 50$. Independent of γ_{\max} , we take $\lambda = k$, since we want to vary only a single parameter in our numerical experiments. When $\gamma_{\max} > 0$, it is possible that $\lambda = 0$ would be a better choice in Method B in some cases [7]. The initial guess is always $m \equiv 0$ (the initial guess used for Examples 1 and 2 often failed for Method A, although it did work for Method B).

First we investigate changing the amount of absorption in the problem for $k_{\max} = 7$, $k_{\min} = 1$. Table 3 shows the results of varying γ_{\max} between 0 and 0.5. As is to be expected, Method B is

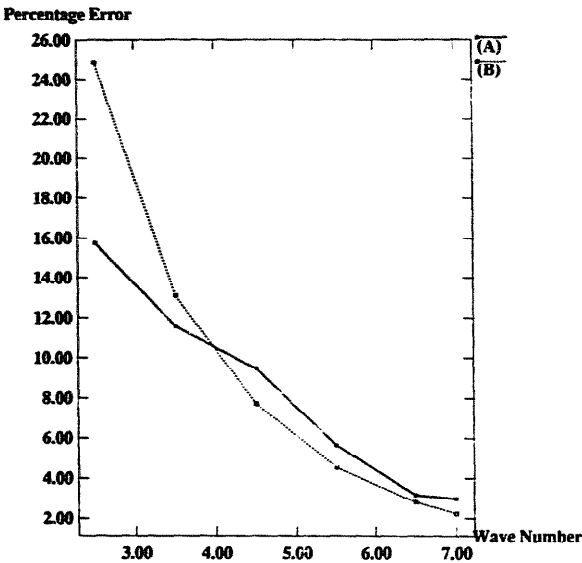


Fig. 1. A graph of the relative L^2 error (4.6) (as a percentage) in the reconstruction of (4.9) and (4.10) as k_{\max} varies. Clearly the reconstruction improves greatly as k_{\max} increases.

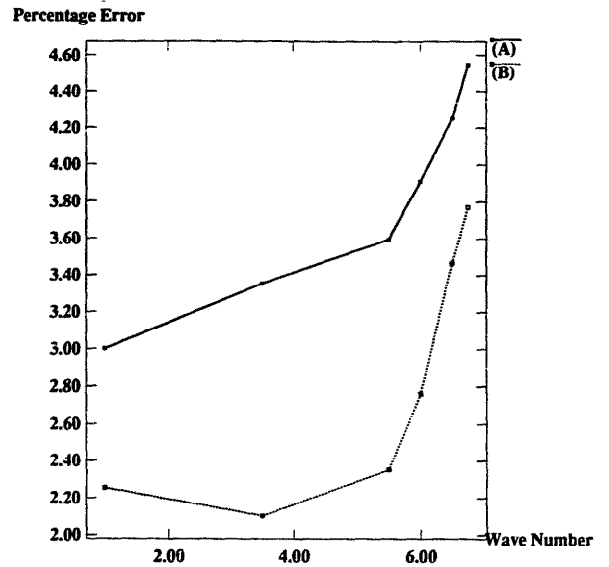


Fig. 2. A graph of the relative L^2 error (4.6) (as a percentage) in the reconstruction of (4.9) and (4.10) as k_{\min} varies. In this case the lower wave numbers contribute little to the quality of the reconstruction.

insensitive to γ_{\max} (although if γ_{\max} is made large enough, we would expect that the quality of reconstruction would deteriorate). Method A does not work for $\gamma_{\max} = 0$. On the basis of numerical evidence, it was suggested in [4] that this failure is due to transmission eigenvalues in $[k_{\min}, k_{\max}]$. The value of γ_{\max} below which Method A is unstable depends on P . For example, when $P = 0$, Method A works satisfactorily when $\gamma_{\max} = 0.15$ but not when $\gamma_{\max} = 0.1$, whereas when $P = 3$, the method works satisfactorily when $\gamma_{\max} = 0.025$ but not when $\gamma_{\max} = 0.01$. These results are the principal reason for preferring Method B over Method A in the case of low absorption.

In [5], we suggested that the poor reconstructions in our examples there might be due to the restrictions on the upper limit on k_{\max} imposed by our finite-element method. Here we investigate the dependence on k_{\max} and k_{\min} of the reconstruction error. Figure 1 shows the relative L^2 error in the reconstruction of (4.9) and (4.10) when $\gamma_{\max} = 0.5$, $k_{\min} = 1$ and k_{\max} varies. Clearly, in this example, increasing k_{\max} greatly improves the reconstruction. This supports our previous claim that problems in [5] were due to low choice of k_{\max} (≈ 4.0).

Figure 2 shows results of the reconstruction of (4.9) and (4.10) with $\gamma_{\max} = 0.5$, $k_{\max} = 7$ and k_{\min} variable. For this example, it is clear that lower wave numbers contribute little information to the reconstruction. However, in the presence of large absorption, the lower wave number may well be important.

References

- [1] D. Colton, *Analytic Theory of Partial Differential Equations* (Pitman, Boston, MA, 1980).
- [2] D. Colton and A. Kirsch, An approximation problem in inverse scattering theory, *Appl. Anal.* **41** (1991) 23–32.
- [3] D. Colton, A. Kirsch and L. Päiväranta, Far field patterns for acoustic waves in an inhomogeneous medium, *SIAM J. Math. Anal.* **20** (1989) 1472–1483.
- [4] D. Colton and P. Monk, The inverse scattering problem for time harmonic acoustic waves in an inhomogeneous medium, *Quart. J. Mech. Appl. Math.* **41** (1988) 97–125.
- [5] D. Colton and P. Monk, The inverse scattering problem for time harmonic acoustic waves in an inhomogeneous medium: numerical experiments, *IMA J. Appl. Math.* **42** (1989) 77–95.
- [6] D. Colton and P. Monk, A new method for solving the inverse scattering problem for acoustic waves in an inhomogeneous medium, *Inverse Problems* **5** (1989) 1013–1026.
- [7] D. Colton and P. Monk, A new method for solving the inverse scattering problem for acoustic waves in an inhomogeneous medium II, *Inverse Problems* **6** (1990) 935–947.
- [8] S.A. Johnson and M.L. Tracy, Inverse scattering solutions by a sinc basis, multiple source, moment method — part I: theory, *Ultrasonic Imaging* **5** (1983) 361–375.
- [9] A. Kirsch, R. Kress, P. Monk and A. Zinn, Two methods for solving the inverse acoustic scattering problem, *Inverse Problems* **4** (1988) 749–770.
- [10] R.E. Kleinman and P.M. van den Berg, A modified gradient method for two-dimensional problems in tomography, *J. Comput. Appl. Math.* **42** (1) (1992) 17–35 (this issue).
- [11] R. Kress, *Linear Integral Equations* (Springer, Berlin, 1989).
- [12] M. Ney, A. Smith and S. Stuchly, A solution of electromagnetic imaging using pseudoinverse transformation, *IEEE Trans. Medical Imaging* **3** (1984) 155–162.
- [13] W. Tabbara, B. Duchêne, Ch. Pichot, D. Lesselier, L. Chommeloux and N. Joachimowicz, Diffraction tomography: contribution to the analysis of some applications in microwaves and ultrasonics, *Inverse Problems* **4** (1988) 305–331.
- [14] M.L. Tracy and S.A. Johnson, Inverse scattering solutions by a sinc basis, multiple source, moment method — part II: numerical evaluations, *Ultrasonic Imaging* **5** (1983) 376–392.

- [15] Y.M. Wang and W.C. Chew, An iterative solution of two dimensional electromagnetic inverse scattering problem, *Internat. J. Imaging Systems Technology* **1** (1989) 100–108.
- [16] Y.M. Wang and W.C. Chew, Reconstruction of permittivity distribution using the Born iterative and distorted Born iterative methods for geophysical applications, in: *Internat. Geoscience and Remote Sensing Conf.*, to appear.
- [17] V.H. Weston, Multifrequency inverse problem for the reduced wave equation with sparse data, *J. Math. Phys.* **25** (1984) 1382–1390.
- [18] V.H. Weston, Multifrequency inverse problem for the reduced wave equation: resolution cell and stability, *J. Math. Phys.* **25** (1984) 3483–3488.